Rare Collision Risk Estimation of Autonomous Vehicles with Multi-Agent Situation Awareness

Zaker, Mahdieh ; Blom, H.A.P.; Soudjani, Sadegh; Lavaei, Abolfazl

Publication date
2024

Document Version
Final published version

Published in
Proceedings of the IEEE 27th Intelligent Transportation Systems Conference (ITSC2024)

Rare Collision Risk Estimation of Autonomous Vehicles with Multi-Agent Situation Awareness

Mahdieh Zaker, *Student Member IEEE*, Henk A.P. Blom, *Fellow IEEE*,
Sadegh Soudjani, *Member IEEE*, and Abolfazl Lavaei, *Senior Member IEEE*

Abstract— **This paper offers a formal framework for the rare collision risk estimation of autonomous vehicles (AVs) with multi-agent situation awareness, affected by different sources of noise in a complex dynamic environment. The estimation framework consists of two complementary parts: modeling formalism and a rare event estimation method using sequential Monte Carlo (MC) simulation instead of importance sampling. By defining incremental levels of severity that must be passed before a collision, a sequence of MC simulations can be applied from one level to the next. This particular sequential MC method consists of the simulation of an Interacting Particle System (IPS) in combination with Fixed Assignment Splitting (FAS) of particles that reach the next level. We model AVs equipped with the situation awareness as *general stochastic hybrid systems* (GSHS), including the IPS-FAS relevant severity levels, and assess the probability of collision in a *lane-change scenario* where two self-driving vehicles simultaneously intend to switch lanes into a shared one while utilizing the *time-to-collision* measure for decision-making as required. The IPS-FAS method is subsequently used to estimate collision risk for this GSHS model of the lane-changing scenario. The results show that in contrast to straightforward MC simulation, IPS-FAS is able to quantify the very low collision risk for the scenario of interest.**

I. Introduction

Autonomous vehicles (AVs) have numerous advantages, including the reduction of air pollution, alleviation of traffic congestion, and mitigation of human-error-related fatalities. However, these complex systems operate within dynamic environments where they interact with a diverse range of factors, presenting various uncertainties, such as unpredictable weather conditions, unexpected pedestrian movements, and the wide-ranging driving behaviors of human operators. AVs are considered safety-critical systems [1] that may pose significant safety risks to human, and ensuring their safe operation in complex and uncertain environments is a paramount challenge.

This challenge involves leveraging information from all agents to enhance AVs' situation awareness (SA) [2]. By doing so, AVs can, in specific scenarios, make informed decisions based on the knowledge of ongoing events [3]. The SA conceptual thinking has originally been developed in the aviation domain [4], which includes modeling a human SA that differs from the truth. More recently, this has been further extended to Multi-Agent SA (MA-SA) relations in a system of multiple agents [5], the origin of which stemmed from the aviation domain [6]. The MA-SA extension makes distinguishing various types of SA differences possible and combines well with [2], [3]. An effective improvement of SA and decision-making by AVs is expected to significantly decrease collision risks. As well explained by [7], it is imperative to quantify the collision risk effect of a particular concept of operation during the design phase.

For an effective design, the collision risk will be so low that quantification through straightforward Monte Carlo simulation becomes too slow [8]. In literature, rare event simulation methods have been developed to handle such cases. The best-known approach is *importance sampling* [9], which involves selecting a sampling distribution and weighting samples by the likelihood ratio between sampling and target distributions. However, finding an appropriate sampling distribution can be challenging, and as the problem dimensions increase, the likelihood ratio becomes less reliable, leading to its avoidance in high-dimensional problems [10]. To avoid these challenges, there is another method known as *importance splitting* [11], also referred to as multi-level splitting [12], or subset simulation [13]. Importance splitting treats rare events as nested occurrences with relatively higher probabilities, focusing on propagating realizations that are likely to lead to the rare event (mutation phase) while discarding others (selection phase) (see *e.g.*, [12], [14]).

An effective way to manage multi-level splitting is to organize it as an *interacting particle system* (IPS) [15], [16]. Unlike the importance sampling method, where both selection and mutation stages are applied to the entire Markov trajectory, IPS applies these stages at various times during the evolution of the Markov process. This IPS approach has successfully been applied to rare event simulation of strong Markov process models of future air traffic designs [17], [18]. Another advantage of the IPS approach is that a significant theory has been developed for particle filtering of strong Markov processes [19]–[21]. By building on this particle filtering background, [22] has proven that the *Fixed Assignment Splitting* (FAS) approach of [23] is most effective in IPS-based rare event estimation for multi-dimensional diffusion processes. Subsequently, [24] has extended this FAS proof to IPS for the much larger class of strong Markov processes used by [17], [18]. In complex multi-agent scenarios, a *compositional data-driven* approach for formally estimating collision risks of AVs with black-box dynamics is introduced in [25].

Original contributions. This paper introduces a formal approach for the rare collision risk estimation of AVs operating on a three-lane road alongside human-driven vehicles by utilizing the interacting particle system-based estimation with fixed assignment splitting (IPS-FAS) algorithm [24]. We model each AV as a general stochastic hybrid system (GSHS) to capture various sources of noise and uncertainty. The specific scenario under examination is shown in Fig. 1: it is a lane-change scenario in which two AVs, green and

M. Zaker and A. Lavaei are with the School of Computing, Newcastle University, United Kingdom. H.A.P Blom is with the Delft University of Technology, The Netherlands. S. Soudjani is with the Max Planck Institute for Software Systems, Germany. Emails: {m.zaker2,abolfazl.lavaei}@newcastle.ac.uk, h.a.p.blom@tudelft.nl, sadegh@mpi-sws.org.

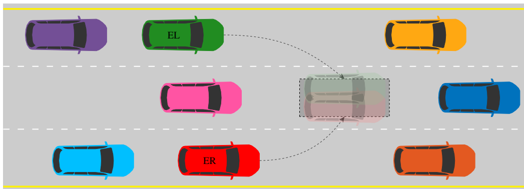

Fig. 1: Lane-change scenario: Two AVs are recognized as $e \in \mathcal{E} = \{EL, ER\}$, with the first letter indicating their status as ego vehicles and the second letter specifying their lane (right or left).

red, are positioned in the first and third lanes amidst human-driven vehicles with an unoccupied space in the second lane. At a specific time instant, both AVs make a decision to change lanes. The concept of operation considered is that when an AV with situation awareness detects the other AV's lane-change intention, it computes the time-to-collision [26] and utilizes this measurement to determine whether to proceed with its lane change or revert to its original lane. Our primary objectives are to compute the potentially *rare collision probability* for these two AVs under different conditions, incorporating situation awareness and computing the time-to-collision measure, and to show that the IPS-FAS approach of [24] is able to quantify the collision risk for this scenario. This can provide effective feedback to the design of the SA and decision-making functions of an AV.

II. General Stochastic Hybrid System Framework

A. Preliminaries and Notation

We denote the set of real and positive real numbers by $\mathbb{R}$ and $\mathbb{R}^+$, respectively, while $\mathbb{N} := \{1, 2, \dots\}$ represents the set of positive integers. The logical AND and OR operations are denoted by $\wedge$ and $\vee$, respectively. Symbols $\mathbf{1}_{n\times m}$ and $\mathbf{0}_{n\times m}$ are matrices of $n \times m$ dimension, consisting of unit and zero elements, respectively. We denote the empty set by $\emptyset$. We use $\mathrm{col}(\cdot)$ to create a vector from its input arguments. Moreover, we denote the exponential distribution with rate parameter λ by $\exp(\lambda)$. The system's state in this work is hybrid, represented by both a continuous variable, denoted as $\mathbf{x}$, and a discrete variable, denoted as θ. The continuous variable evolves in some open sets in Euclidean space X^θ, while the discrete variable is an element of a countable set Θ. The hybrid state space is denoted by $\Xi \triangleq \bigcup_{\theta\in\Theta}\{\theta\}\times X^\theta$, and $\overline{\Xi} = \Xi \cup \partial\Xi$ represents the closure of Ξ, where $\partial\Xi \triangleq \bigcup_{\theta\in\Theta}\{\theta\} \times \partial X^\theta$ is the boundary of Ξ.

We consider a probability space $(\Omega, \mathcal{F}_\Omega, \mathbb{P}_\Omega)$, where Ω is the sample space, $\mathcal{F}_\Omega$ is a σ-algebra on Ω comprising subsets of Ω as events, and $\mathbb{P}_\Omega$ is a probability measure that assigns probabilities to events. Let $(\mathbb{W}_s)_{s\geq 0}$ be an m-dimensional $\mathbb{F}$-Brownian motion, and $(\mathbb{P}_s)_{s\geq 0}$ be an m'-dimensional $\mathbb{F}$-Poisson process (mutually independent). If X is a Hausdorff topological space, $\mathcal{B}(X)$ denotes its Borel σ-algebra, and $(X, \mathcal{B}(X))$ is a Borel space.

B. GSHS Definition

As autonomous vehicles (AVs) operate in a complex environment interacting with various entities, they might face numerous unpredicted events. Henceforth, different sources of uncertainty should be taken into account when modeling AVs. To do so, we employ the notion of general stochastic hybrid systems, which encompasses a wide range of stochastic phenomena, as follows [27].

Definition 2.1 (GSHS): Each agent of AVs is modeled as a general stochastic hybrid system (GSHS), denoted by $\mathcal{A} = \big((\Theta, d, \mathcal{X}), f, g, Init, \lambda, R\big)$, where

- Θ is a countable set of discrete variables;
- $d : \Theta \to \mathbb{N}$ is a mapping that provides the dimensions of the continuous state spaces for each element in Θ;
- $\mathcal{X} : \Theta \to \mathbb{R}^{d(\cdot)}$ associates each $\theta \in \Theta$ with an open subset X^θ within $\mathbb{R}^{d(\theta)}$;
- $f : \Xi \to \mathbb{R}^{d(\cdot)}$ is a vector field;
- $g : \Xi \to \mathbb{R}^{d(\cdot)\times m}$ is an $X^{(\cdot)}$-valued matrix, $m \in \mathbb{N}$;
- $Init : \mathcal{B}(\Xi) \to [0, 1]$ is an initial probability measure on $(\Xi, \mathcal{B}(\Xi))$;
- $\lambda : \overline{\Xi} \to \mathbb{R}^+$ is a transition rate function;
- $R : \overline{\Xi} \times \mathcal{B}(\overline{\Xi}) \to [0, 1]$ is a transition measure.

Then, a stochastic process $\{\theta_t, \mathbf{x}_t\}$ is called a GSHS execution if there exists a sequence of stopping times $s_0 = 0 < s_1 < s_2 < \cdots$ such that for each $j \in \mathbb{N}$,

- $(\theta_0, \mathbf{x}_0)$ is a Ξ-valued random variable extracted according to the probability measure $Init$;
- For $t \in [s_{j-1}, s_j)$, θ_t, $\mathbf{x}_t$ is a solution of the stochastic differential equation (SDE):
$$\begin{cases} \mathsf{d}\theta_t = 0 \\ \mathsf{d}\mathbf{x}_t = f(\theta_t, \mathbf{x}_t)\mathsf{d}t + g(\theta_t, \mathbf{x}_t)\mathsf{d}\mathbb{W}_t \end{cases}$$
in which $\mathbb{W}_t$ is an m-dimensional standard Brownian motion.
- s_j is the minimum of the following two stopping times:
  (i) first hitting time $t > s_{j-1}$ of the boundary of $X^{\theta_{s_{j-1}}}$ by the phase process $\{\mathbf{x}_t\}$;
  (ii) first moment $t > s_{j-1}$ of a transition event to happen at rate $\lambda(\theta_t, \mathbf{x}_t)$.
- At the stopping time s_j the hybrid state $(\theta_{s_j}, \mathbf{x}_{s_j})$ meets the conditional probability measure $p_{\theta_{s_j}, \mathbf{x}_{s_j}|\theta_{s_j-}, \mathbf{x}_{s_j-}}(A|\theta, \mathbf{x}) = R((\theta, \mathbf{x}), A)$ for all $A \in \mathcal{B}(\Xi)$, where s_j- indicates the time instant immediately before the stopping time s_j is reached.

C. Transformation to SHS

According to [28], a GSHS can be transformed to an SHS, as a *more tractable model*, involving four key modifications:

(i) An auxiliary state component q_t, representing "remaining local time", is initialized at a specific stopping time τ with an initial condition of $q_\tau \sim \exp(1)$;
(ii) The exit boundary of X^θ is expanded by introducing an additional boundary condition, where $q_{t-} = 0$, *i.e.,* the value of q_t just before t;
(iii) Spontaneous probabilistic jumps in $\{\theta_t, \mathbf{x}_t\}$ are replaced by forced probabilistic jumps occurring at the moment when $q_{t-} = 0$;
(iv) When the extended exit boundary is reached at the stopping time τ', the "remaining local time" is resampled as $q_{\tau'} \sim \exp(1)$.

Subsequently, the GSHS $\mathcal{A} = \big((\Theta, d, \mathcal{X}), f, g, Init, \lambda, R\big)$ is transformed to the SHS $\mathcal{A}^* = \big((\Theta^*, d^*, \mathcal{X}^*), f^*, g^*, Init^*, R^*\big)$ as follows:

- $\Theta^* = \Theta$, $d^* = d + 1$, $\mathcal{X}^* = \mathcal{X} \times (0, \infty)$;
- $f^*(\theta_t, \mathbf{x}_t, \cdot) = \big[f(\theta_t, \mathbf{x}_t) \quad -\lambda(\theta_t, \mathbf{x}_t)\big]^\top$;
- $g^*(\theta_t, \mathbf{x}_t, \cdot) = \big[g(\theta_t, \mathbf{x}_t) \quad 0\big]^\top$;

- $Init^* = \big[Init \quad q_0\big]^\top$ with $q_0 \sim \exp(1)$;
- $R^*\big((\theta_t, \mathbf{x}_t, \cdot); A \times \mathsf{d}q\big) = R\big((\theta_t, \mathbf{x}_t); A\big) \times e^{-q}\mathsf{d}q$.

This transformation is mainly helpful for system execution (cf. Algorithm 2), upon which one can estimate the rare event probability (cf. Algorithm 1). Having delved into the general stochastic hybrid system for modeling AVs, in pursuit of our goal to enhance the safety of AVs in the lane-change scenario, we leverage a *multi-agent situation awareness* framework in the following section.

III. Multi-Agent Situation Awareness

Here, we leverage the concept of multi-agent situation awareness (MA-SA), building upon the fundamental work in [5]. In a multi-agent system of N agents $\mathcal{A}_i,\ i \in \{1, \ldots, N\}$, each agent has state $z_{t,i}$ at time instant t, comprising of SA and non-SA states. The multi-agent situation awareness relation of agent $\mathcal{A}_i$ regarding agent $\mathcal{A}_j$ is represented by Z_i^j, which is a set of N_i^j different pairs $(s, r)_n,\ n \in \{1, \ldots, N_i^j\}$ such that s references state element $z_{t,i}(s)$ and r references state element $z_{t,j}(r)$. Subsequently, the SA of agent $\mathcal{A}_i$ about the state of agent $\mathcal{A}_j$ at time instant t is represented by $\sigma_{t,i}^j$ as follows:

$$\sigma_{t,i}^j \triangleq \big\{z_{t,i}(s),\ \exists r \text{ s.t. } (s, r) \in Z_i^j\big\}. \tag{1}$$

It can be concluded that non-empty Z_i^j leads to non-empty $\sigma_{t,i}^j$, which means agent $\mathcal{A}_i$ possesses SA about agent $\mathcal{A}_j$. In addition to the MA-SA components $\sigma_{t,i}^j,\ j \neq i$, $\zeta_{t,i}$ denotes *base state* of $\mathcal{A}_i$, determining state elements of $z_{t,i}$ that are not in relation with any other state element through $\{Z_i^j,\ j = 1, \ldots, N\}$, *i.e.*,

$$\zeta_{t,i} \triangleq \big\{z_{t,i}(s),\ \text{s.t. } (s, r) \notin Z_i^j \text{ for } \forall (j, r)\big\}. \tag{2}$$

Following (1)-(2), the state $z_{t,i}$ of agent $\mathcal{A}_i$ contains base state $\zeta_{t,i}$ and SA of other agents $\sigma_{t,i}^j,\ j \neq i$, as

$$z_{t,i} = \zeta_{t,i} \bigcup_{j \neq i} \sigma_{t,i}^j. \tag{3}$$

IV. IPS-based Rare-event Simulation

Here, we estimate the probability γ of the hybrid system states $(\theta_t, \mathbf{x}_t)$, reaching a closed subset $D \subset \Xi$ within a finite time interval $[0, T]$, defined as

$$\gamma = \mathbb{P}(\tau < T), \tag{4}$$

where τ is the first time that $\{\theta_t, \mathbf{x}_t\}$ enters the set D, *i.e.*,

$$\tau = \inf\{t > 0, (\theta_t, \mathbf{x}_t) \in D\}. \tag{5}$$

A. IPS-FAS Algorithm

The approach to factorizing the reach probability, denoted as γ, involves the introduction of a sequence denoted as $D_k, k \in \{0, \ldots, m\}$, comprising nested closed subsets within the domain Ξ. More precisely, we define $D = D_m \subset D_{m-1} \subset \cdots \subset D_1 \subset D_0 = \Xi$, with the specific condition that D_1 is chosen to ensure $\mathbb{P}\{(\theta_0, \mathbf{x}_0) \in D_1\} = 0$. Furthermore, to represent the first time instant at which the pair $(\theta_t, \mathbf{x}_t)$ enters the region D_k, τ_k is defined as

$$\tau_k = \inf\{t > 0; (\theta_t, \mathbf{x}_t) \in D_k \vee t \geq T\}. \tag{6}$$

To attain the desired factorization, we employ $\{0, 1\}$-valued random variables $\chi_k,\ k \in \{0, \ldots, m\}$, defined as

$$\chi_k = \begin{cases} 1, & \text{if } \tau_k < T, \\ 0, & \text{otherwise.} \end{cases} \tag{7}$$

Algorithm 1: IPS-FAS algorithm for a GSHS

Input: Initial measure π_0, end time T, decreasing sequence of closed subsets $D_k = \{(\theta_t, \mathbf{x}_t) \in \Xi\}$, $D_{k-1} \supset D_k,\ k \in \{1, \ldots, m\}$. Also $D_0 = \Xi$, $Q_k = (0, T) \times D_k$ and number of particles N_P

Output: Estimated reach probability $\bar{\gamma}$

0. Initiation: Generate N_P particles
$\xi_0^i \sim \pi_0,\ i \in \{1, \ldots, N_P\}$,
i.e. $\bar{\pi}_0(\cdot) = \sum_{i=1}^{N_P} \frac{1}{N_P} \delta_{\{\xi_0^i\}}(\cdot)$, with Dirac δ. Set $k = 1$

I. Mutation (Algorithm 2):
for $i = 1, \ldots, N_P$ **do**
  $\bar{\xi}_k^i = \texttt{Execute}(\xi_{k-1}^i)$
end
Then, $\bar{p}_k(\cdot) = \sum_{i=1}^{N_P} \frac{1}{N_P} \delta_{\{\bar{\xi}_k^i\}}(\cdot)$

II. Conditioning:
$\bar{\gamma}_k = \frac{N_{S_k}}{N_P}$ with $N_{S_k} = \sum_{i=1}^{N_P} 1(\bar{\xi}_k^i \in Q_k)$
if $N_{S_k} = 0$ **then**
  $\bar{\gamma}_{k'} = 0,\ k' \in \{k, \ldots, m\}$ and go to Step **V**
end

III. Selection: $\tilde{\pi}_k(\cdot) = \frac{1}{N_{S_k}} \sum_{i=1}^{N_{S_k}} \delta_{\{\tilde{\xi}_k^i\}}(\cdot)$, with $\{\tilde{\xi}_k^j\}_{j=1}^{N_{S_k}}$ the collection of $\bar{\xi}_k^i \in Q_k,\ i \in \{1, \ldots, N_P\}$

IV. Splitting: $\{\tilde{\tilde{\xi}}_k^j\}_{j=1}^{N_{S_k}}$ is a random permutation of $\{\tilde{\xi}_k^j\}_{j=1}^{N_{S_k}}$
for $i = 1, \ldots, N_{S_k}$ **copy**

$$\text{Step I}: \begin{cases} \xi_k^i & = \tilde{\tilde{\xi}}_k^i \\ \xi_k^{N_{S_k}+i} & = \tilde{\tilde{\xi}}_k^i \\ \vdots & \vdots \\ \xi_k^{(\lfloor N_P/N_{S_k} \rfloor - 1)N_{S_k}+i} & = \tilde{\tilde{\xi}}_k^i \end{cases}$$

end
for $i = 1, \ldots, N_P - \lfloor N_P/N_{S_k} \rfloor N_{S_k}$ **copy**

$$\text{Step II}: \quad \xi_k^{\lfloor N_P/N_{S_k} \rfloor N_{S_k}+i} = \tilde{\tilde{\xi}}_k^i$$

end
Each particle receives weight $1/N_P$

V. if $\bar{\gamma}_k \neq 0$ **then**
  if $k < m$, **then**
    $k := k + 1$ and go to Step I (Mutation)
  else
    $\bar{\gamma} = \prod_{k=1}^{m} \bar{\gamma}_k$
  end
else
  $\bar{\gamma} = 0$
end

The factorization presented in the following proposition holds significant practical value by which the reach probability γ is expressed as a product of individual probabilities γ_k. This factorization allows us to systematically explore and estimate the contribution of each level D_k to the overall rare-event probability.

Proposition 4.1: The factorization is satisfied by the reach probability

$$\gamma = \prod_{k=1}^{m} \gamma_k, \tag{8}$$

where $\gamma_k \triangleq \mathbb{E}\big\{\chi_k = 1 \,\big|\, \chi_{k-1} = 1\big\} = \mathbb{P}\big(\tau_k < T \,\big|\, \tau_{k-1} < T\big)$.

By using the strong Markov property of $\{\theta_t, \mathbf{x}_t\}$, one can develop a recursive estimation of γ using the factorization in (8) with $\Xi' \triangleq \mathbb{R} \times \Xi$, $\xi_k \triangleq (\tau_k, \theta_{\tau_k}, \mathbf{x}_{\tau_k})$, $Q_k \triangleq (0, T) \times D_k$, for $k \in \{1, \ldots, m\}$, and the conditional probability measure $\pi_k(B) \triangleq \mathbb{P}(\xi_k \in B | \xi_k \in Q_k)$, for an arbitrary Borel set B

of Ξ'. A solution to the recursion of transformations is given by π_k as follows [16]:

$$\pi_{k-1}(\cdot) \xrightarrow{\text{I. mutation}} p_k(\cdot) \xrightarrow{\text{III. selection}} \pi_k(\cdot)$$
$$p_k(\cdot) \;\big\downarrow\; \text{II. conditioning} \quad \gamma_k$$

where $p_k(B) \triangleq \mathbb{P}(\xi_k \in B | \xi_{k-1} \in Q_{k-1})$. By employing the same approach, the following algorithmic steps outline the numerical estimation of γ using the IPS method:

$$\overline{\pi}_{k-1}(\cdot) \xrightarrow{\text{I. mutation}} \overline{p}_k(\cdot) \xrightarrow{\text{III. selection}} \tilde{\pi}_k(\cdot) \xrightarrow{\text{IV. splitting}} \overline{\pi}_k(\cdot)$$
$$\overline{p}_k(\cdot) \;\big\downarrow\; \text{II. conditioning} \quad \overline{\gamma}_k$$

Here, $\overline{\gamma}_k$, $\overline{p}_k$, and $\overline{\pi}_k$ indicate empirical density approximations of γ_k, p_k, and π_k, each of which is formed employing a set of N_P particles. Those particles that succeed in reaching Q_k from Q_{k-1} form $\tilde{\pi}_k$. Here, four steps must be taken to estimate the reach probability γ, including *mutation*, *conditioning*, *selection*, and *splitting*. The *mutation* step consists of executing the SHS $\mathcal{A}^*$, where system equations are evaluated at time t until the next time instant $t_+ = \min\{t+\Delta, \bar{s}_t, \bar{\tau}_k\}$, in which Δ is a small time step, $\bar{s}_t$ is the first time $> t$ that the solution hits the boundary of X^*, and $\bar{\tau}_k$ is the first time that the solution hits $Q_k^* = Q_k \times \mathbb{R}$. This evaluation is repeated until it hits the next level set Q_k and the successful particles are collected. This execution is outlined in Algorithm 2. The *conditioning* step is calculating the ratio of N_{S_k} successful particles reaching Q_k to N_P particles, resulting the reach probability $\bar{\gamma}_k$ which is zero if $N_{S_k} = 0$. In the *selection* step, the successful particles are selected to be used in the *splitting* step, which is copying each of the N_{S_k} successful particles as extensively as feasible. The approach used in *splitting* step is the fixed assignment splitting, which consists of two steps. In Step I, each particle is copied $\lfloor N_P/N_{S_k} \rfloor$ times, while in Step II, the remaining $N_P - \lfloor N_P/N_{S_k} \rfloor N_{S_k}$ particles are chosen randomly (without replacement) from N_{S_k} particles and added to the ones from Step I. Then, these steps are repeated until $\bar{\gamma}_k$, $\forall k \in \{1, \ldots, m\}$ are obtained, and ultimately, the estimated reach probability $\bar{\gamma}$ is calculated (cf. Algorithm 1).

B. Enrich GSHS with IPS Levels

As explained in Subsection II-C, a GSHS can be transformed into an SHS, the simulation of which is simpler. However, as has been explained in [24], the "remaining local time" process $\{q_t\}$ of the SHS transformed version of a GSHS should be treated as being unobservable for the IPS process. To formalize this, [24] proposed to first enrich the GSHS model with the IPS hitting levels Q_k, $k \in \{1, \ldots, m\}$, and with the reset $(\theta_{\tau_k}, \mathbf{x}_{\tau_k}) = (\theta_{\tau_k -}, \mathbf{x}_{\tau_k -})$ at a hitting time τ_k. Thanks to the continuity of the latter reset, the execution of the enriched GSHS yields the same pathwise solutions as the execution of the original GSHS does. Subsequent application of the transformation of Subsection II-C to this enriched GSHS yields an enriched SHS, which also resets the remaining local time upon reaching an IPS hitting level Q_k, $k \in \{1, \ldots, m\}$. In Algorithm 2, this enrichment is reflected in the reset of the local remaining time at the beginning of each IPS cycle (Step 1) through a fresh sampling from $\exp(1)$.

The combination of Algorithms 1 and 2 starts at each IPS cycle with N_P particles, each of which has a different sample

---

Algorithm 2: The execution function of SHS

Input: Particle vector $\xi_{k-1} = (\tau_{k-1}, \theta^*_{\tau_{k-1}}, \mathbf{x}^*_{\tau_{k-1}}, q^*_{\tau_{k-1}})$, SHS elements $(\Theta^*, d^*, X^*, f^*, g^*, Init^*, R^*)$, and $Q_k^* = Q_k \times \mathbb{R}$

Output: Estimated particle $\bar{\xi}_k = (\bar{\tau}_k, \bar{\theta}^*_{\bar{\tau}_k}, \bar{\mathbf{x}}^*_{\bar{\tau}_k}, \bar{q}^*_{\bar{\tau}_k})$

Function $\bar{\xi}_k$ = `Execute(`ξ_{k-1}`)`**:**

1 Set $t := \tau_{k-1}$ and $\bar{\varsigma} := (\theta^*_{\tau_{k-1}}, \mathbf{x}^*_{\tau_{k-1}}, \bar{q})$, with $\bar{q} \sim \exp(1)$

2 Evaluate equation (9) for the AVs and $\mathsf{d}q_t/\mathsf{d}t = -\lambda(\theta_t, \mathbf{x}_t)$ from $\bar{\varsigma}$ at t until $t_+ = \min\{t+\Delta, \bar{s}_t, \bar{\tau}_k\}$; this yields $\bar{\varsigma}_+$

3 **if** $t_+ \geq \bar{\tau}_k$ **then**
- $\bar{\xi}_k = (\bar{\tau}_k, \bar{\theta}^*_{\bar{\tau}_k}, \bar{\mathbf{x}}^*_{\bar{\tau}_k}, \bar{q}^*_{\bar{\tau}_k})$, where
- **if** $\bar{s}_t = \bar{\tau}_k$ **then**
  - $(\bar{\theta}^*_{\bar{\tau}_k}, \bar{\mathbf{x}}^*_{\bar{\tau}_k}, \bar{q}^*_{\bar{\tau}_k}) \sim R^*(\bar{\varsigma}_+, \cdot)$
- **else**
  - $(\bar{\theta}^*_{\bar{\tau}_k}, \bar{\mathbf{x}}^*_{\bar{\tau}_k}, \bar{q}^*_{\bar{\tau}_k}) := \bar{\varsigma}_+$
- **end**

end

4 **if** $t_+ \geq \bar{s}_t$ **then**
- $\bar{\varsigma} \sim R^*(\bar{\varsigma}_+, \cdot)$, set $t := t_+$ and repeat from Step 2

end

end

---

of remaining local time $q^*_{\tau_{k-1}}$. Without the enrichment of SHS with the IPS levels, the N_P particles would only have different remaining local time q^*_0 at the start of the first IPS cycle. As demonstrated in [24], particle diversity increases with the rising IPS level k, thanks to this enrichment.

The next step is to specify a GSHS for the scenario to be considered, as explained below.

> **Scenario:** Consider two AVs $i, j \in \mathcal{E}$, driving in the first and third lanes of a three-lane highway, each is followed by another vehicle while also following a leading one. There is a free spot in the second lane, as illustrated in Fig. 1, and there exists a specific moment in time when both vehicles decide to change lanes. Quantify the *potentially rare collision probability* γ of these two subject vehicles by assuming that ER possesses SA and is modeled as a GSHS.

V. Our Framework through a Case Study

For the sake of better illustration of the underlying concept and technicality, we present a running case study which utilizes the model of a vehicle for AVs $\mathcal{E}$.

A. Ego Vehicles Modeling

We consider the following 5D model, adapted from [29], for each ego vehicle $i \in \mathcal{E}$:

$$\begin{aligned}
\mathsf{d}x_{t,i} &= (v_{x_i}\cos(\vartheta_{t,i}) - v_{y_{t,i}}\sin(\vartheta_{t,i}))\mathsf{d}t + \varepsilon_1 \mathsf{d}\mathbb{P}_t + \varepsilon_2 \mathsf{d}\mathbb{W}_t, \\
\mathsf{d}y_{t,i} &= (v_{x_i}\sin(\vartheta_{t,i}) + v_{y_{t,i}}\cos(\vartheta_{t,i}))\mathsf{d}t + \varepsilon_1 \mathsf{d}\mathbb{P}_t + \varepsilon_2 \mathsf{d}\mathbb{W}_t, \\
\mathsf{d}\vartheta_{t,i} &= \omega_{t,i}\mathsf{d}t, \\
\mathsf{d}v_{y_{t,i}} &= (\frac{F_{yf}}{m}\cos(u_{t,i}) + \frac{F_{yr}}{m} - v_{x_i}\omega_{t,i})\mathsf{d}t, \\
\mathsf{d}\omega_{t,i} &= (\frac{L_f}{I_z}F_{yf}\cos(u_{t,i}) - \frac{L_r}{I_z}F_{yr})\mathsf{d}t,
\end{aligned} \tag{9}$$

where $x_{t,i}$ and $y_{t,i}$ are the positions of the vehicle's center of gravity in x and y directions, respectively, $\vartheta_{t,i}$ is the vehicle's orientation, $v_{y_{t,i}}$ is the velocity in the y direction whereas v_{x_i} is the constant velocity in the x direction, $\omega_{t,i}$ is the yaw rate, $\mathbb{P}_t$ is a Poisson process with rate λ_1 and reset term ε_1, and $\mathbb{W}_t$ is a Brownian motion with diffusion term ε_2. The only control input is the front wheel steering angle $u_{t,i}$. Note that since this work is concerned with the verification problem, not controller synthesis, this control input is assumed to be already designed and deployed to the vehicle. The primary objective here is to conduct analysis and compute the rare collision risk probability. Incorporating the stiffness coefficients for front and rear tires $C_{\alpha f}$ and $C_{\alpha r}$, respectively, the forces acting on the front and rear tires F_{yf} and F_{yr}, assuming a linear tire model, can be expressed as

$$F_{yf} = -C_{\alpha f}\alpha_f, \quad F_{yr} = -C_{\alpha r}\alpha_r,$$

where the two slip angles α_f and α_r are as

$$\alpha_f = \frac{v_{y_{t,i}} + L_f\omega_{t,i}}{v_{x_i}} - u_{t,i}, \quad \alpha_r = \frac{v_{y_{t,i}} - L_r\omega_{t,i}}{v_{x_i}},$$

with L_f and L_r being the distance from the vehicle's center of gravity to the front and rear wheels.

The components of the GSHS model can be determined according to Definition 2.1 as follows:

$$\begin{aligned} f(\theta_{t,i}, \mathbf{x}_{t,i}) = \text{col}\big(&v_{x_i}\cos(\vartheta_{t,i}) - v_{y_{t,i}}\sin(\vartheta_{t,i}),\\ &v_{x_i}\sin(\vartheta_{t,i}) + v_{y_{t,i}}\cos(\vartheta_{t,i}), \omega_{t,i},\\ &\frac{F_{yf}}{m}\cos(u_{t,i}) + \frac{F_{yr}}{m} - v_{x_i}\omega_{t,i},\\ &\frac{L_f}{I_z}F_{yf}\cos(u_{t,i}) - \frac{L_r}{I_z}F_{yr}\big), \end{aligned} \tag{10a}$$

$$g(\theta_{t,i}, \mathbf{x}_{t,i}) = \varepsilon_2 \ \text{col}\left(\mathbf{1}_{2\times1}, \mathbf{0}_{3\times1}\right), \tag{10b}$$

where $\mathbf{x}_{t,i} = \text{col}(x_{t,i}, y_{t,i}, \vartheta_{t,i}, v_{y_{t,i}}, \omega_{t,i})$.

In order to model ER with continuous states $\mathbf{x}_{t,ER}$ described by (9) as a GSHS model, we should first determine the discrete states $\theta_{t,ER}$. To this aim, we define $\underline{\theta}_{t,ER} \in \underline{\Theta}_{ER}$ as the *modes of driving* where

$$\underline{\Theta}_{ER} = \{0, 1, 2, -1, Hit\},$$

in which each component indicates when the AV ER

- 0: is moving straight, 1: is changing lanes;
- 2: is aware of the other vehicle changing lanes;
- -1: is changing its decision (changing lanes in the opposite direction, *i.e.*, returning to its previous lane);
- Hit: collides with the other vehicle.

Then, we define $\upsilon_t \in \Upsilon$ which indicates the *intent of the vehicle*, with set Υ being defined as

$$\Upsilon = \{Off, 1^+, 1^-\},$$

in which each component indicates:

- Off: when the indicators of the AV is off and it is likely not to change lanes;
- 1^+: when the right indicator of the AV is flashing and it is changing its lane to the corresponding lane;
- 1^-: when the left indicator of the AV is flashing and it is changing its lane to the corresponding lane.

Discrete state of the AV ER is $\theta_{t,ER} = (\underline{\theta}_{t,ER}, \upsilon_t) \in \Theta_{ER}$, with Θ_{ER} as follows:

$$\Theta_{ER} = \big\{(0, Off), (1, 1^-), (2, 1^-), (-1, 1^+), (Hit, \star)\big\},$$

where, the element denoted by $\star$ is non-contributory, meaning that its value has no impact on the outcome. Analogously, we define discrete states $\theta_{t,EL}$ of the other AV. However, since EL is assumed *not to have SA*, the modes 2 and -1 are not applicable for it. Therefore, $\underline{\theta}_{t,EL} \in \underline{\Theta}_{EL}$ with $\underline{\Theta}_{EL} = \{0, 1, Hit\}$. Hence, $\theta_{t,EL} = (\underline{\theta}_{t,EL}, \upsilon_t) \in \Theta_{EL}$, with Θ_{EL} defining as

$$\Theta_{EL} = \big\{(0, Off), (1, 1^+), (Hit, \star)\big\}.$$

B. MA-SA Modeling

Now that the AVs are modelled, we can define MA-SA relations for AV ER. To this aim, we define the continuous-valued SA state vector as

$$\hat{\mathbf{x}}_{t,ER}^{EL} = \text{col}(\hat{x}_{t,EL}, \hat{y}_{t,EL}, \hat{\vartheta}_{t,EL}, \hat{v}_{y_{t,EL}}), \tag{11}$$

and *augment* it with $\mathbf{x}_{t,ER}$, resulting in continuous-valued state vector with SA $z_{t,ER} = \text{col}\left(\mathbf{x}_{t,ER}, \hat{\mathbf{x}}_{t,ER}^{EL}, \eta_{t,ER}\right) \in \mathbb{R}^{10}$, in which $\eta_{t,ER}$ indicates the amount of time passed since the AV ER becomes aware of the other's intention to change its lane. Thus, Z_{ER}^{EL} is defined as

$$\begin{aligned} Z_{ER}^{EL} &= \big\{(6,1), (7,2), (8,3), (9,4)\big\}\\ &= \big\{\hat{x}_{t,EL}, \hat{y}_{t,EL}, \hat{\vartheta}_{t,EL}, \hat{v}_{t,EL}\big\}. \end{aligned}$$

Similarly, the augmented *discrete*-valued state vector with SA is

$$\breve{\theta}_{t,ER} = \text{col}\left(\theta_{t,ER}, \hat{\theta}_{t,ER}^{EL}\right), \tag{12}$$

where $\theta_{t,ER} \in \Theta_{ER}$ and $\hat{\theta}_{t,ER}^{EL} \in \Theta_{EL}$. Hence, the GSHS model of the AV ER has *hybrid states* $(\breve{\theta}_{t,ER}, z_{t,ER})$. The augmented continuous states $z_{t,ER}$ evolve within the switching moments of $\{\breve{\theta}_{t,ER}\}$ as

$$\breve{f}(\breve{\theta}_{t,ER}, z_{t,ER}) = \text{col}\left(f(\theta_{t,ER}, \mathbf{x}_{t,ER}), \hat{f}(\hat{\theta}_{t,ER}^{EL}, \hat{\mathbf{x}}_{t,ER}^{EL}), 1\right),$$

where $f(\theta_{t,ER}, \mathbf{x}_{t,ER})$ is as in (10a), and $\hat{f}(\hat{\theta}_{t,ER}^{EL}, \hat{\mathbf{x}}_{t,ER}^{EL})$ is as follows:

$$\begin{aligned} &\hat{f}(\hat{\theta}_{t,ER}^{EL}, \hat{\mathbf{x}}_{t,ER}^{EL}) =\\ &\quad \text{col}\big(v_{x_{EL}}\cos(\hat{\vartheta}_{t,EL}) - \hat{v}_{y_{t,EL}}\sin(\hat{\vartheta}_{t,EL}),\\ &\quad v_{x_{EL}}\sin(\hat{\vartheta}_{t,EL}) + \hat{v}_{y_{t,EL}}\cos(\hat{\vartheta}_{t,EL}), \omega_{t,EL},\\ &\quad \frac{F_{yf}}{m}\cos(u_{t,EL}) + \frac{F_{yr}}{m} - v_{x_{EL}}\omega_{t,EL}\big). \end{aligned} \tag{13}$$

In addition, for hybrid states $(\breve{\theta}_{t,ER}, z_{t,ER})$, we define

$$\breve{g}(\breve{\theta}_{t,ER}, z_{t,ER}) = \text{col}\left(g(\theta_{t,ER}, \mathbf{x}_{t,ER}), \hat{g}(\hat{\theta}_{t,ER}^{EL}, \hat{\mathbf{x}}_{t,ER}^{EL}), 0\right),$$

in which $g(\theta_{t,ER}, \mathbf{x}_{t,ER})$ is as in (10b), and $\hat{g}(\hat{\theta}_{t,ER}^{EL}, \hat{\mathbf{x}}_{t,ER}^{EL}) = \mathbf{0}_{4\times1}$.

Remark 5.1: Another discrete-state SA that can be generally considered is the *identity of vehicles*. This information can be obtained as initial data from the object and treated as a time-invariant state, incorporated into the vehicle's decision-making process.

C. Splitting Levels in IPS

Since both vehicles are moving, reaching static level sets D_k, $k \in \{0, \ldots, m\}$, detailed in Section IV, is not applicable anymore. To deal with this problem, we consider a *set of ellipses* around each AV of the following form

$$\mathcal{O}_{k,i} := \Big\{\frac{(x - x_{t,i})^2}{r_{x_k}^2} + \frac{(y - y_{t,i})^2}{r_{y_k}^2} = 1 \Big| k \in \{1, \ldots, m\}\Big\}, \tag{14}$$

where r_{x_k} and r_{y_k} are the primary axes, and $(x_{t,i}, y_{t,i})$, with $i \in \mathcal{E}$, is the center of each ellipse. Then, we determine whether $\mathcal{O}_{k,i} \cap \mathcal{O}_{k,j} \neq \emptyset$, for $i, j \in \mathcal{E}$, $i \neq j$. This

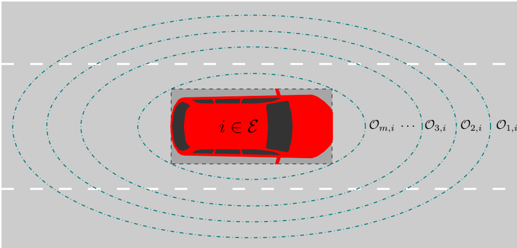

Fig. 2: Ellipsoidal level sets $\mathcal{O}_{k,i}$ as in (14) around each AV.

demonstrates that the AVs are getting closer to each other and that they might collide. To be more precise, the intersection of the last ellipses, *i.e.*, $\mathcal{O}_{m,i} \cap \mathcal{O}_{m,j} \neq \emptyset$, for $i, j \in \mathcal{E}$, $i \neq j$, means that the accident has happened. We choose $\mathcal{O}_{m,i}$ to be a circumscribed ellipse, *i.e.*, the tightest one around the AVs, with primary axes $r_{x_m} = \mathcal{R}_x = \frac{\sqrt{2}}{2} l_v$ and $r_{y_m} = \mathcal{R}_y = \frac{\sqrt{2}}{2} w_v$, with l_v and w_v being the length and width of the vehicle, respectively. It is noteworthy that the ellipses are nested subsets within the domain Ξ as well, *i.e.*, $\mathcal{O}_i = \mathcal{O}_{m,i} \subset \mathcal{O}_{m-1,i} \subset \cdots \subset \mathcal{O}_{1,i} \subset \mathcal{O}_{0,i} \subseteq \Xi$. This setting of level sets is depicted in Fig. 2.

As long as the AV EL is not close enough to the AV ER so that it can receive the necessary information for situation awareness, we assume the AV ER is not aware of the AV EL. To demonstrate this behavior, we consider the ellipse $\mathcal{O}_{SA,i}$ as defined in (14) as the area of awareness around each AV with primary axes μ_{r_x} and μ_{r_y}. Whenever the awareness ellipses of the two AVs intersect, *i.e.*, $\mathcal{O}_{SA,i} \cap \mathcal{O}_{SA,j} \neq \emptyset$, the AV ER becomes aware of the other AV and can receive information for (11) and (12). Upon recognizing the presence of EL, if $\hat{\theta}^{EL}_{t,ER} = (1, 1^+)$, *i.e.*, EL is changing lane, it will take ER some time to transit to $\theta_{t,ER} = (2, 1^-)$ and decide for its next move. This *delay* can be modeled as an *instantaneous transition rate* $\lambda_2(\check{\theta}_{t,ER}, z_{t,ER})$ which satisfies

$$\lambda_2(\check{\theta}, z) = \chi\big(\theta_{t,ER} = (1, 1^-)\big)\, p_{delay}(\eta) \Big/ \int_{\eta}^{\infty} p_{delay}(s) \mathrm{d}s, \tag{15}$$

where $p_{delay}(s) = \frac{s}{\mu_d^2} e^{-s^2/(2\mu_d^2)}$, with the mean reaction delay μ_d being a Rayleigh density.

D. Ego Decision-making

Upon obtaining data from the SA vector (11) of a neighboring vehicle, the ego vehicle must determine its course of action in the event of a potential collision. Time-related measures can be used as a cue for decision making, one of which is time-to-collision (TTC) measure. A shorter TTC indicates a higher risk of collision. The TTC for a vehicle α at a given moment t, concerning a preceding vehicle $\alpha - 1$, following the same path, can be computed using

$$\mathrm{TTC}_{\alpha} = \frac{x_{t,\alpha-1} - x_{t,\alpha} - l_{\alpha-1}}{v_{t,\alpha} - v_{t,\alpha-1}}, \ \forall v_{t,\alpha} > v_{t,\alpha-1}, \tag{16}$$

where l is the length of the vehicle [30]. Different modifications have been made to (16) in various studies. An innovative method is recently proposed in [31] for computing TTC in both car-following and lane-change scenarios by incorporating the equation of motion and vehicle direction. To do so, the category of the collision is firstly identified as either angular or rear-end, with the latter occurring frequently in car-following scenarios. The type of collision is determined by the angle between the movement trajectories of two vehicles, which is represented as a vector whose start and end points are the vehicle's coordinates at the previous and current time instants, respectively. The movement angle of each vehicle can be calculated as provided in Table I.

Algorithm 3: Determining the predicted collision point between two vehicles

Input: Current coordinates $(x_{0,\mathtt{sub}}, y_{0,\mathtt{sub}})$ and $(x_{0,\mathtt{col}}, y_{0,\mathtt{col}})$ of the subject and colliding vehicles

Output: The common collision point (c_x, c_y), if it exists

Construct the equation of two lines as the motion path of each vehicle using their current position coordinates $(x_{0,\mathtt{sub}}, y_{0,\mathtt{sub}})$ and $(x_{0,\mathtt{col}}, y_{0,\mathtt{col}})$:

$$y_{t,\mathtt{sub}} = x_{t,\mathtt{sub}} \tan\varphi_{\mathtt{sub}} + (y_{0,\mathtt{sub}} - x_{0,\mathtt{sub}} \tan\varphi_{\mathtt{sub}})$$
$$y_{t,\mathtt{col}} = x_{t,\mathtt{col}} \tan\varphi_{\mathtt{col}} + (y_{0,\mathtt{col}} - x_{0,\mathtt{col}} \tan\varphi_{\mathtt{col}})$$

Find the intersection of the lines:

$$y_{t,\mathtt{sub}} = y_{t,\mathtt{col}} \longrightarrow \begin{cases} x_{\mathtt{sub}} = x_{\mathtt{col}} = c_x, \\ y_{\mathtt{sub}} = y_{\mathtt{col}} = c_y \end{cases}$$

Solve the following equations for t:

$$\begin{cases} c_x = x_{0,\mathtt{sub}} + \sum_{n=1}^{k} \left(\frac{1}{n!} \times \frac{\partial^n x_{t,\mathtt{sub}}}{\partial t^n} \times t^n \right), & k \in \mathbb{N} \\ c_x = x_{0,\mathtt{col}} + \sum_{n=1}^{k} \left(\frac{1}{n!} \times \frac{\partial^n x_{t,\mathtt{col}}}{\partial t^n} \times t^n \right), & k \in \mathbb{N} \end{cases}$$

$$\begin{cases} c_y = y_{0,\mathtt{sub}} + \sum_{n=1}^{k} \left(\frac{1}{n!} \times \frac{\partial^n y_{t,\mathtt{sub}}}{\partial t^n} \times t^n \right), & k \in \mathbb{N} \\ c_y = y_{0,\mathtt{sub}} + \sum_{n=1}^{k} \left(\frac{1}{n!} \times \frac{\partial^n y_{t,\mathtt{col}}}{\partial t^n} \times t^n \right), & k \in \mathbb{N} \end{cases}$$

if $t \in \mathbb{R}^+$ *for each of the four equation exists* **then**
  (c_x, c_y) is the predicted collision point and $\mathrm{TTC}_{\mathtt{sub}}$ can be calculated for this point
else
  There is no predicted collision point and $\mathrm{TTC}_{\mathtt{sub}} = \infty$
end

TABLE I: Calculating the angle of motion for each vehicle.

Condition	Angle φ
$x_2 > x_1$, $y_2 > y_1$	$\arctan\left\lvert \frac{y_2 - y_1}{x_2 - x_1} \right\rvert$
$x_2 < x_1$, $y_2 > y_1$	$\pi - \arctan\left\lvert \frac{y_2 - y_1}{x_2 - x_1} \right\rvert$
$x_2 < x_1$, $y_2 < y_1$	$\pi + \arctan\left\lvert \frac{y_2 - y_1}{x_2 - x_1} \right\rvert$
$x_2 > x_1$, $y_2 < y_1$	$2\pi - \arctan\left\lvert \frac{y_2 - y_1}{x_2 - x_1} \right\rvert$

If the angle of a prospective collision, which is the absolute difference between the angles of motion of two vehicles, falls between -10 and $+10$ degrees and both vehicles are traveling in the same lane, the conflict is considered a rear-end collision. The necessary and sufficient condition for rear-end collision is as follows:

$$x_{t,\alpha} - x_{t,\alpha-1} + l_{\alpha-1} = 0 \iff \text{Rear-end collision.} \tag{17}$$

Assuming the $(k-1)^{\text{th}}$ derivative of velocity is constant, we can derive an approximate equation of motion for each vehicle as follows:

Algorithm 4: TTC calculation for angular conflicts

Input: Predicted collision point for the subject vehicle, *i.e.*, $(x_{t,\mathtt{sub}}, y_{t,\mathtt{sub}}) = (c_x, c_y)$ and its current location $(x_{0,\mathtt{sub}}, y_{0,\mathtt{sub}})$
Output: $\mathrm{TTC}_{\mathtt{sub}}$ for the subject vehicle

1 Calculate the distance between the current location of the subject vehicle and the predicted collision point: $d_{\mathtt{sub}} = \sqrt{(c_x - x_{0,\mathtt{sub}})^2 + (c_y - y_{0,\mathtt{sub}})^2}$

2 Calculate time to the predicted collision point based on the type of motion:
$$d_{\mathtt{sub}} = \frac{\sum_{n=1}^{k}\left(\frac{1}{n!} \times \frac{\partial^n x_{t,\mathtt{sub}}}{\partial t^n} \times t^n\right)}{\cos\varphi_{\mathtt{sub}} \text{ or } \sin\varphi_{\mathtt{sub}}}$$

3 **if** $\exists i \in \{1,\ldots,k\},\ t_i \notin \mathbb{R}^+$ **then**
  $\mathrm{TTC}_{\mathtt{sub}} = \infty$
else
  $\mathrm{TTC}_{\mathtt{sub}} = \min\{t_i \in \mathcal{T} | t_i \in \mathbb{R}^+\}$
end

$$\begin{cases} x_{t,\alpha} = x_{0,\alpha} + \sum_{n=1}^{k}\left(\frac{1}{n!} \times \frac{\partial^n x_{t,\alpha}}{\partial t^n} \times t^n\right), \\ x_{t,\alpha-1} = x_{0,\alpha-1} + \sum_{n=1}^{k}\left(\frac{1}{n!} \times \frac{\partial^n x_{t,\alpha-1}}{\partial t^n} \times t^n\right). \end{cases} \tag{18}$$

Combining (17) and (18) results in the k^{th} degree polynomial

$$x_{0,\alpha} - x_{0,\alpha-1} + l_{\alpha-1} + \sum_{n=1}^{k}\left(\frac{1}{n!} \times \left[\frac{\partial^n x_{t,\alpha}}{\partial t^n} - \frac{\partial^n x_{t,\alpha-1}}{\partial t^n}\right] \times t^n\right) = 0, \tag{19}$$

whose solution is $\mathcal{T} = \{t_1, t_2, \ldots, t_k\}$. Then,

$$\mathrm{TTC}_k = \min\{t_i \in \mathcal{T} | t_i \in \mathbb{R}^+\}, \tag{20}$$

implying that TTC_k is the minimum, non-zero and real solution of (19).

When dealing with angular collisions, the initial step involves ascertaining whether a subject vehicle "sub" and a colliding vehicle "col" share a common collision point, at which TTC can be calculated. In order to compute the common collision point, the motion path of each vehicle is determined by constructing line equations for each based on their calculated angles, as in Step 1 of Algorithm 3. The intersection of these lines results in the point (c_x, c_y), which might be the common collision point according to (21). Then, the motion type of each vehicle is determined by examining their previous positions in x and y directions at each time instant:

$$\begin{cases} x_{t,\mathtt{sub}} = x_{0,\mathtt{sub}} + \sum_{n=1}^{k}\left(\frac{1}{n!} \times \frac{\partial^n x_{t,\mathtt{sub}}}{\partial t^n} \times t^n\right), & k \in \mathbb{N}, \\ y_{t,\mathtt{sub}} = y_{0,\mathtt{sub}} + \sum_{n=1}^{k}\left(\frac{1}{n!} \times \frac{\partial^n y_{t,\mathtt{sub}}}{\partial t^n} \times t^n\right), & k \in \mathbb{N}, \end{cases} \tag{21a}$$

$$\begin{cases} x_{t,\mathtt{col}} = x_{0,\mathtt{col}} + \sum_{n=1}^{k}\left(\frac{1}{n!} \times \frac{\partial^n x_{t,\mathtt{col}}}{\partial t^n} \times t^n\right), & k \in \mathbb{N}, \\ y_{t,\mathtt{col}} = y_{0,\mathtt{col}} + \sum_{n=1}^{k}\left(\frac{1}{n!} \times \frac{\partial^n y_{t,\mathtt{col}}}{\partial t^n} \times t^n\right), & k \in \mathbb{N}. \end{cases} \tag{21b}$$

We solve (21a) and (21b) at the point (c_x, c_y) for t and then examine the solutions. If $t \in \mathbb{R}^+$, then the point (c_x, c_y) is considered as the common collision point. The necessary steps to specify the collision point are given in Algorithm 3. Then, if a common collision point exists, TTC for the subject vehicle can be determined. To this aim, the distance $d_{\mathtt{sub}}$ between the subject vehicle and the collision point (c_x, c_y) resulting from Algorithm 3 is calculated. Then, we calculate the time it takes the subject vehicle to drive this distance, either in the x or y direction. This results in a set of solutions, $\mathcal{T} = \{t_1, t_2, \ldots, t_k\}$, with k being the order of the motion equation, for which we check whether all t in $\mathcal{T}$ are *real and positive*. If this condition is satisfied, the minimum t in $\mathcal{T}$ is TTC; otherwise, no collision will occur. This procedure is outlined in Algorithm 4. In the process of TTC computation, the subject vehicle utilizes the information provided by the SA vector (11).

When the AV ER is in making decision mode $(2, 1^-)$, indicating awareness of another AV changing lanes, it calculates the TTC measure to determine whether to complete its maneuver or change its decision and return to its own lane (transition to mode $(-1, 1^+)$). We consider a threshold TTC_{th} so that if $\mathrm{TTC}_{ER} \leq \mathrm{TTC}_{\text{th}}$, completing the maneuver is hazardous and the AV ER will go back to its own lane. The transition graphs of the completed GSHS models for AVs $i = ER$ and $j = EL$ are provided in Figs. 3a and 3b, respectively.

VI. Simulation Results and Discussions

In order to utilize Algorithm 1, we first need to define the level sets as described in (14). We assume each AV has six ellipses around it with the primary axes $r_{x_k} = r_k\mathcal{R}_x$ and $r_{y_k} = r_k\mathcal{R}_y$ for all $k \in \{1, \ldots, 6\}$, where $r_1 = 2$ and the declining rate is 0.2, leading to $r_6 = 1$. The parameters of the AVs described by (9) are set as $v_{x_i} = 20\,m/s$, $\varepsilon_1 = 10^{-6}$, $\varepsilon_2 = 10^{-2}$, $\lambda_1 = 0.5$, $m = 2000\,kg$, $I_z = 2000\,kgm^2$, $C_{\alpha f} = C_{\alpha r} = 6 \times 10^4$, $L_f = L_r = 2\,m$, $l_v = 4.508\,m$, and $w_v = 1.61\,m$. To perform a lane-change maneuver, we utilize a simple PD controller of the form $u_{t,i} = K_p\big(y_{d,i} - y_{t,i}\big) - K_d\frac{\mathrm{d}y_{t,i}}{\mathrm{d}t}$ with $K_p = 1.5\times10^{-3}$, $K_d = 10^{-2}$, and $y_{d,i}$ is the desired position in the y direction. In the scenario under study, we set $w_L = 3.5\,m$, $\mu_d = 0.6\,s$, and $\mathrm{TTC}_{\text{th}} = 10\,s$.

Our aim is to analyze the effect of the area of awareness $\mathcal{O}_{SA,ER}$, based on the different values of μ_r in $\mu_{r_x} = \mu_r\mathcal{R}_x$ and $\mu_{r_y} = \mu_r\mathcal{R}_y$. To increase the reliability of the outcomes, we run the scenario $\mathcal{N}$ times and get the results $\bar{\gamma}_n$, $n \in \{1, \ldots, \mathcal{N}\}$. Then, we report the *mean probability* $\hat{\gamma} = \frac{\sum_{n=1}^{\mathcal{N}} \bar{\gamma}_n}{\mathcal{N}}$ as the estimated probability of reaching $\mathcal{O}_{6,ER} \cap \mathcal{O}_{6,EL} \neq \emptyset$. We report our obtained results in Table II with $\mathcal{N} = 100$ trials and $N_P = 100$ particles for Algorithm 1 and the corresponding Monte-Carlo (MC) simulation for the sake of comparison.

The highlights of simulation results can be considered threefold, which are given below:

- The scenario's parameters are considered in a way that an accident occurs in the absence of SA;
- Given that an accident occurs in this scenario due to the lack of SA, it becomes evident how SA plays a crucial role in reducing accident risk. Furthermore, Table II illustrates that even minor adjustments in SA parameters can significantly affect collision probabilities;
- Finally, Table II underscores the superiority of the IPS-FAS algorithm over MC simulation. While MC yields a zero probability outcome, IPS-FAS provides a probability on the order of 10^{-7}, highlighting its precision. Given that AVs belong to safety-critical systems, the precision of calculations within their decision-making is of vital importance.

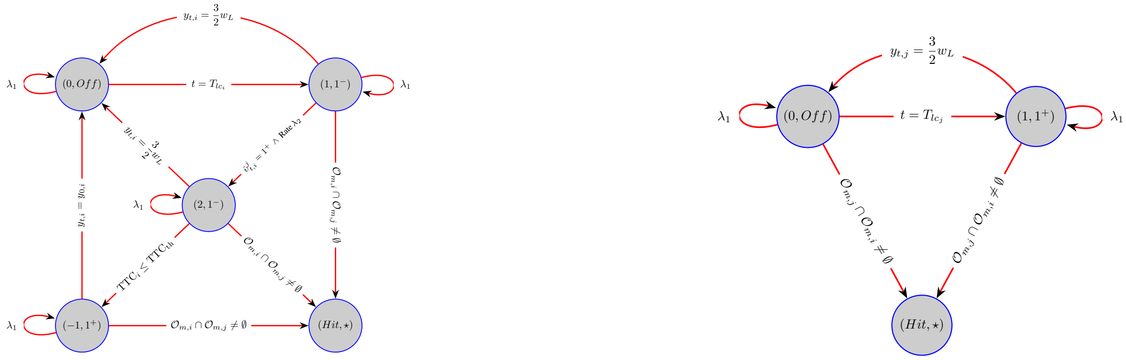

(a) (b)

Fig. 3: GSHS model transition graphs for AVs $i = ER$ (a), and $j = EL$ (b), where, w_L represents lane width, and T_{lc_i}, T_{lc_j} signify moments when vehicles i and j decide to change lanes, respectively. The intent $\hat{v}^j_{t,i}$ is obtained from $\hat{\theta}^j_{t,i}$.

TABLE II: The value of mean probability $\hat{\gamma}$ for various μ_r using Algorithm 1 and MC (m = 1).

Algorithm	μ_r				
	1.5825	1.6275	1.6725	1.7	1.7375
IPS-FAS	1.9131×10^{-4}	8.6350×10^{-5}	7.6300×10^{-6}	2.8725×10^{-6}	5.4320×10^{-7}
MC	1.8000×10^{-4}	7.9000×10^{-5}	0	0	0

REFERENCES

[1] J. C. Knight, "Safety critical systems: challenges and directions," in *Proceedings of the 24th International Conference on Software Engineering*, 2002, pp. 547–550.

[2] A. Wardziński, "Safety assurance strategies for autonomous vehicles," in *Proceedings of International Conference on Computer Safety, Reliability, and Security*. Springer, 2008, pp. 277–290.

[3] ——, "The role of situation awareness in assuring safety of autonomous vehicles," in *Proceedings of the International Conference on Computer Safety, Reliability, and Security*. Springer, 2006, pp. 205–218.

[4] M. R. Endsley, "Toward a theory of situation awareness in dynamic systems," *Human factors*, vol. 37, no. 1, pp. 32–64, 1995.

[5] H. A. Blom and A. Sharpanskykh, "Modelling situation awareness relations in a multiagent system," *Applied Intelligence*, vol. 43, pp. 412–423, 2015.

[6] S. Stroeve, H. Blom, and M. Van der Park, "Multi-agent situation awareness error evolution in accident risk modelling," 2003.

[7] J. Reich and M. Trapp, "SINADRA: towards a framework for assurable situation-aware dynamic risk assessment of autonomous vehicles," in *Proceedings of the 16th European Dependable Computing Conference (EDCC)*. IEEE, 2020, pp. 47–50.

[8] N. Metropolis and S. Ulam, "The Monte Carlo method," *Journal of the American Statistical Association*, vol. 44, no. 247, pp. 335–341, 1949.

[9] J. A. Bucklew and J. Bucklew, *Introduction to rare event simulation*. Springer, 2004, vol. 5.

[10] Z. I. Botev and D. P. Kroese, "An efficient algorithm for rare-event probability estimation, combinatorial optimization, and counting," *Methodology and Computing in Applied Probability*, vol. 10, pp. 471–505, 2008.

[11] P. Glasserman, P. Heidelberger, P. Shahabuddin, and T. Zajic, "Multilevel splitting for estimating rare event probabilities," *Operations Research*, vol. 47, no. 4, pp. 585–600, 1999.

[12] P. L'Ecuyer, F. Le Gland, P. Lezaud, and B. Tuffin, "Splitting techniques," *Rare event simulation using Monte Carlo methods*, pp. 39–61, 2009.

[13] S.-K. Au and J. L. Beck, "Estimation of small failure probabilities in high dimensions by subset simulation," *Probabilistic engineering mechanics*, vol. 16, no. 4, pp. 263–277, 2001.

[14] J. Morio and M. Balesdent, *Estimation of rare event probabilities in complex aerospace and other systems: a practical approach*. Woodhead publishing, 2015.

[15] P. Del Moral and J. Garnier, "Genealogical particle analysis of rare events," 2005.

[16] F. Cérou, P. Del Moral, F. Le Gland, and P. Lezaud, "Genetic genealogical models in rare event analysis," Ph.D. dissertation, INRIA, 2006.

[17] H. A. Blom, J. Krystul, and G. Bakker, "A particle system for safety verification of free flight in air traffic," in *Proceedings of the 45th Conference on Decision and Control (CDC)*. IEEE, 2006, pp. 1574–1579.

[18] H. A. Blom, J. Krystul, G. Bakker, M. B. Klompstra, and B. K. Obbink, "Free flight collision risk estimation by sequential MC simulation," *Stochastic Hybrid Systems*, pp. 249–281, 2007.

[19] A. Doucet, N. De Freitas, and N. J. Gordon, *Sequential Monte Carlo methods in practice*. Springer, 2001, vol. 1, no. 2.

[20] P. Del Moral, M. Kouritzin, and L. Miclo, "On a class of discrete generation interacting particle systems," 2001.

[21] M. Gerber, N. Chopin, and N. Whiteley, "Negative association, ordering and convergence of resampling methods," *The Annals of Statistics*, vol. 47, no. 4, pp. 2236–2260, 2019.

[22] H. Ma and H. A. P. Blom, "Random assignment versus fixed assignment in multilevel importance splitting for estimating stochastic reach probabilities," *Methodology and Computing in Applied Probability*, vol. 24, no. 4, pp. 2313–2338, 2022.

[23] M. J. Garvels and D. P. Kroese, "A comparison of RESTART implementations," in *1998 Winter Simulation Conference. Proceedings (Cat. No. 98CH36274)*, vol. 1. IEEE, 1998, pp. 601–608.

[24] H. Ma and H. A. Blom, "Interacting particle system based estimation of reach probability of general stochastic hybrid systems," *Nonlinear Analysis: Hybrid Systems*, vol. 47, 2023.

[25] A. Lavaei, L. Di Lillo, A. Censi, and E. Frazzoli, "Formal estimation of collision risks for autonomous vehicles: A compositional data-driven approach," *IEEE Transactions on Control of Network Systems*, vol. 10, no. 1, pp. 407–418, 2022.

[26] D. Greene, J. Liu, J. Reich, Y. Hirokawa, A. Shinagawa, H. Ito, and T. Mikami, "An efficient computational architecture for a collision early-warning system for vehicles, pedestrians, and bicyclists," *IEEE Transactions on Intelligent Transportation Systems*, vol. 12, no. 4, pp. 942–953, 2011.

[27] M. L. Bujorianu and J. Lygeros, "Toward a general theory of stochastic hybrid systems," *Stochastic hybrid systems: theory and safety critical applications*, pp. 3–30, 2006.

[28] J. Lygeros and M. Prandini, "Stochastic hybrid systems: a powerful framework for complex, large scale applications," *European Journal of Control*, vol. 16, no. 6, pp. 583–594, 2010.

[29] R. Pepy, A. Lambert, and H. Mounier, "Path planning using a dynamic vehicle model," in *Proceedings of the 2nd International Conference on Information & Communication Technologies*, vol. 1. IEEE, 2006, pp. 781–786.

[30] M. M. Minderhoud and P. H. L. Bovy, "Extended time-to-collision measures for road traffic safety assessment," *Accident Analysis & Prevention*, vol. 33, no. 1, pp. 89–97, 2001.

[31] N. Nadimi, D. R. Ragland, and A. Mohammadian Amiri, "An evaluation of time-to-collision as a surrogate safety measure and a proposal of a new method for its application in safety analysis," *Transportation letters*, vol. 12, no. 7, pp. 491–500, 2020.